ChemElectroChem

Articles
doi.org/10.1002/celc.202100020

Chemistry Europe
European Chemical
Societies Publishing

Electrografted Interfaces on Metal Oxide Electrodes for Enzyme Immobilization and Bioelectrocatalysis

Tomos G. A. A. Harris,[a, b] Nina Heidary,[a, b, c] Stefan Frielingsdorf,[b] Sander Rauwerdink,[d] Abbes Tahraoui,[d] Oliver Lenz,[b] Ingo Zebger,*[b] and Anna Fischer*[a, b, e, f]

In this work, we demonstrate that diazonium electrografting of biocompatible interfaces on transparent conducting oxide indium tin oxide (ITO) can be controlled and optimized to achieve low charge transfer resistance, allowing highly efficient electron transfer to an immobilized model enzyme, the oxygen-tolerant [NiFe]-hydrogenase from *Ralstonia eutropha*. The use of a radical scavenger enables control of the interface thickness, and thus facilitates maximization of direct electron transfer processes between the enzyme's active center and the electrode. Using this approach, amine and carboxylic acid functionalities were grafted on ITO, allowing enzyme immobili-

zation both under moderate electrostatic control and covalently via amide bond formation. Despite an initial decrease in catalytic activity, covalent immobilization led to an improvement in current stability compared to just electrostatically immobilized enzyme. Given the superior stability of electrografted interfaces in comparison to adsorbed or self-assembled interfaces, we propose electrografting as an alternative approach for the functional immobilization of redox-active enzymes on transparent conducting oxide (TCO) electrodes in bioelectronic devices.

1. Introduction

Transparent conducting oxide electrodes (e.g. tin doped indium oxide (ITO),[1–5] antimony doped tin oxide (ATO)[6–10] as well as titanium dioxide (TiO$_2$)[11,12]) are gaining more and more attention as electrodes in the field of bioelectrocatalysis. TCO electrodes exhibit many characteristics that make them suitable

[a] Dr. T. G. A. A. Harris, Dr. N. Heidary, Prof. Dr. A. Fischer
     Albert-Ludwigs-Universität Freiburg
     Institut für Anorganische und Analytische Chemie
     Albertstr. 21, 79104 Freiburg, Germany
     E-mail: anna.fischer@ac.uni-freiburg.de
[b] Dr. T. G. A. A. Harris, Dr. N. Heidary, Dr. S. Frielingsdorf, Dr. O. Lenz,
     Dr. I. Zebger, Prof. Dr. A. Fischer
     Technische Universität Berlin
     Institut für Chemie, PC 14
     Str. des 17. Juni 135, 10623 Berlin, Germany
     E-mail: ingo.zebger@tu-berlin.de
[c] Dr. N. Heidary
     Department of Chemistry
     Université de Montréal
     Roger-Gaudry Building, Montreal, Quebec H3C 3J7, Canada
[d] S. Rauwerdink, Dr. A. Tahraoui
     Paul-Drude-Institut für Festkörperelektronik
     Hausvogteiplatz 5–7, 10117 Berlin, Germany
[e] Prof. Dr. A. Fischer
     Freiburger Materialforschungszentrum (FMF)
     Albert-Ludwigs-Universität Freiburg
     Stefan-Meier-Straße 21, 79104 Freiburg, Germany
[f] Prof. Dr. A. Fischer
     FIT Freiburger Zentrum für interaktive Werkstoffe und bioinspirierte Technologien
     Georges-Köhler-Allee 105, 79110 Freiburg, Germany

     Supporting information for this article is available on the WWW under
     https://doi.org/10.1002/celc.202100020

as electrode materials in bioelectronic devices, e.g. enzymatic fuel cells and biosensors, including ease of fabrication using a broad range of synthetic techniques, tunable porosities/surface areas, low-costs, high stabilities under physiological conditions, broad electrochemical potential range as well as high biocompatibility.[7,9,13–18] Moreover, their transparency facilitates their use in artificial photosynthesis,[5,19,20] wearable electronics,[18] and spectroelectroanalysis,[1,2,21] while their favorable dielectric properties can also be utilized in biosupercapacitors.[22,23] Amongst different TCOs, ITO has a high conductivity and transparency as well as a wide electrochemical stability window at neutral pH (-0.6 to $+2$ V *vs*. SHE, pH 7.0),[24] making it a suitable electrode material for electrochemical,[1,2] photoelectrochemical[4,5,19,20,25] as well as spectroelectrochemical applications[1,2,21] with redox active proteins and enzymes. In addition, porous ITO electrodes with high surface areas and a wide range of pore sizes (from mesoporous to macroporous scaffolds) have been reported in literature,[1,2,4,26] allowing the immobilization of high electroactive loadings of proteins and enzymes; an important factor for a lot of bioelectronic and bioelectrocatalytic devices.

In all of these devices, it may be necessary to use chemically modified electrodes to influence the electrostatic, hydrophobic and van der Waals interactions between the electrode and the amino acid building blocks of the enzyme. This is done to prevent desorption of the protein molecules, as well as to control their orientation on the surface to maximize electron transfer (ET) to catalytic centers, e.g. by direct "wiring", and to thereby maximize the performance of the final device.[27] Direct electron transfer (DET) between redox enzymes and electrodes is often complicated by the insulating protein shell of the enzymes and thereby results in the need to orient the intra-enzymatic electron transfer chain or active site at a distance ideally below 1.4 nm from the electrode to enable efficient

ChemElectroChem

Articles
doi.org/10.1002/celc.202100020

**Chemistry
Europe**
European Chemical
Societies Publishing

electron tunneling.[27,28] As a result, significant efforts have been devoted to understanding and optimizing the interaction between electrode materials and enzymes.[6,27,29–33]

Anchoring groups commonly used for chemically attaching organic functional groups to oxides (e.g. phosphonates, carboxylates, silanes etc.) either suffer from limited stabilities or poor electronic coupling with the electrode.[34–37] Recently, we have demonstrated that electrografting aryl-diazonium salts onto antimony-doped tin oxide (ATO) electrodes resulted in robust, covalently-bound interfaces that are stable in a very broad pH and potential range, and facilitated fast ET with an immobilized molecular electrocatalyst, such as an iron Hangman porphyrin.[38] Further studies demonstrated similarly high stabilities of such electrografted interfaces on tin-doped indium oxide (ITO), fluorine-doped tin oxide (FTO) and TiO_2.[37,39–41] The reactive aryl radicals, formed during electrografting, tend, however, to react with already-grafted species, resulting in the deposition of polymeric, branched interfaces that do not facilitate DET with, e.g., large redox enzymes. Unlike small molecules, enzymes cannot penetrate such structures. While electrografting has previously been used to immobilize redox enzymes on electrode materials such as carbon and gold in an electroactive manner,[42–48] this has to the best of our knowledge not been successfully extended to TCO materials so far. A recent study described the immobilization of a redox enzyme on electrografted ITO, albeit in a non-electroactive manner.[41]

The addition of radical scavengers during electrografting has been demonstrated as a simple and effective way of suppressing polymerization and favoring monolayer formation on carbon materials.[49–52] Similar effects in terms of grafting control towards optimized interfaces have been obtained by us for gold, enabling, e.g., tuning of the interfacial charge transfer resistance thereby allowing to enhance the reactivity of immobilized electrocatalytic molecular species.[31] In the present work, we demonstrate that controlled electrografting leading to improve interfaces with low charge transfer resistance is also achievable on ITO. Taking advantage of this effect, we deposited amine- and carboxylic-functionalized interfaces (bearing small amounts of positive and negative charges, respectively) of varying thicknesses on ITO. We demonstrate how they can be used to optimize the electrostatic immobilization of a model redox enzyme, the oxygen-tolerant membrane-bound [NiFe]-hydrogenase of *Ralstonia eutropha* (MBH), to maximize DET and catalytic currents. We then used the modified electrodes to covalently attach the enzyme and demonstrate an increase in stability, albeit at the expense of diminished catalytic activity.

We show for the first time highly efficient immobilization of a redox-active enzyme on a TCO in an electroactive manner, using diazonium electrografting, and propose this as an improved method for immobilizing enzymes on TCO-based bioelectrodes.

2. Results and Discussion

2.1. Interface Formation on ITO using Electrografting in the Presence of a Radical Scavenger

Diazonium salts have been successfully electrografted on a number of planar and porous oxide materials, where it is assumed that M–O–C interfacial bonds are formed, as has been proven for TiO_2 and ATO,[37,38] and indications of (extensive) polymerization are reported.[41] The first step was therefore to determine the effect of adding radical scavenger to the electrografting reaction and the thereby deposited interfaces. Highly conductive and reproducibly planar ITO electrodes were used to study the electrochemical interface, ruling out potential charge carrier transport limitations found in porous materials, as well as diffusion limitations and more complex surface chemistries within porous structures. A similar approach to that used by Menanteau et al.[52] on carbon electrodes was employed in here for ITO electrodes. Nitrophenyl (Ph–NO_2) groups were thereby electrografted on the ITO working electrode from an acetonitrile solution of 4-nitrobenzene diazonium tetrafluoroborate (4-NBD) containing increasing molar equivalents of the radical scavenger 2,2-diphenyl-1-picrylhydrazyl (DPPH), which allows (sub)-monolayer coverages to be obtained.

Figure 1 summarizes the charge transfer resistances (R_{CT}) of the modified and unmodified ITO electrodes as well as the surface coverages of the Ph–NO_2 species (Γ_{NO_2}). R_{CT} has been determined by electrochemical impedance spectroscopy (EIS) in the presence of $Fc^{0/+}$ (SI, Figure S1) while Γ_{NO_2} has been estimated by measuring the charge consumed during their electrochemical reduction to aminophenyl (Ph–NH_2) species using CV in protic media (Figure 2). The R_{CT} provides an indication of the density of the deposited interfaces.

Briefly, the reduction of Ph–NO_2 groups in protic media proceeds via an irreversible 4 e^- reduction to hydroxyamino-
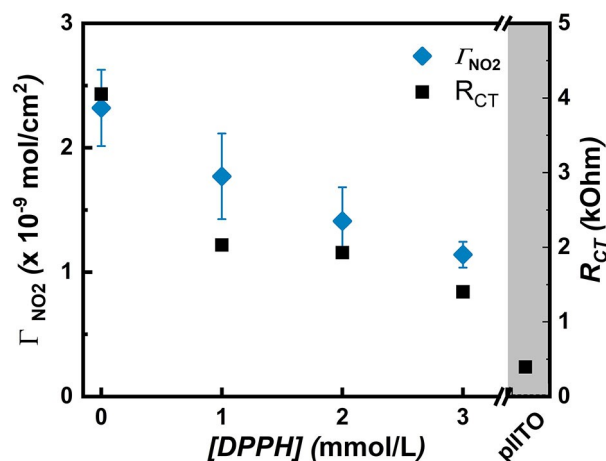

Figure 1. Charge transfer resistances R_{CT} for ITO electrodes electrografted with Ph–NO_2 species in the presence of increasing amounts of the radical scavenger DPPH, as well as the corresponding surface coverages Γ_{NO_2} of Ph–NO_2 species are plotted. For comparison, the charge transfer resistance R_{CT} for unmodified ITO electrodes was also determined (shaded area of the plot). All working electrodes had the same geometric surface area of 0.4 cm^2.
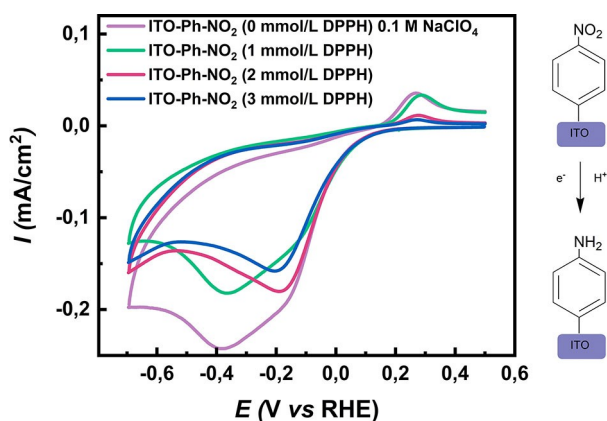
ChemElectroChem

Articles
doi.org/10.1002/celc.202100020

Chemistry
Europe

European Chemical
Societies Publishing

Figure 2. First CVs showing the electrochemical reduction of Ph–NO$_2$ moieties in various Ph–NO$_2$ interfaces, which were electrografted on ITO with increasing DPPH concentrations in the deposition electrolyte. Reaction carried out in 0.1 mol/L NaClO$_4$ (under Ar) using a scan rate of 50 mVs^{-1}.

phenyl groups (Ph–NHOH), which can further be reduced to Ph–NH$_2$ via an irreversible 2 e$^-$ reduction. Remaining Ph–NHOH species that are not fully reduced to Ph–NH$_2$ can subsequently be reversibly oxidized to nitrosophenyl groups (Ph–NO). For details on this reaction and the method used to calculate Γ_{NO_2}, see the work of Brooksby et al.[53]

An increase in R$_{CT}$ (compared to unmodified pl-ITO) is observed after electrografting Ph–NO$_2$ interfaces in the absence of DPPH, as expected after the formation of a relatively thick/dense organic interface. The value of R$_{CT}$ decreases sharply in case that the electrografting was performed in the presence of 1 mmol/L DPPH, and the values of R$_{CT}$ continue to decrease with increasing DPPH concentrations, albeit to a lesser extent. This decrease in R$_{CT}$ as a function of increasing DPPH concentration correlates with a decrease in Γ_{NO_2}. The behavior observed here is thus similar to that observed by Menanteau et al. on glassy carbon and indicates that polymerization is suppressed by the addition of radical scavenger.[52] We observed a similar behavior on Au and antimony doped tin electrodes in our previous studies.[31,38] For this to happen, the rate of the phenyl radical coupling to the electrode surface must be greater than the rate of coupling with the scavenger, whereas the rate of phenyl radical coupling with the already grafted moieties must be smaller. When this is not the case, less dense, albeit still polymeric interfaces are deposited in the presence of a radical scavenger, as we were able to show for Au electrodes.[31] It should be noted that Γ_{NO_2} for thick films are often significantly underestimated using the electrochemical reduction method described above due to some Ph–NO$_2$ moieties remaining redox inactive/incompletely reduced.[53,54]

Figure 2 shows cyclic voltammograms (CVs) resulting from electrochemical reduction of nitro groups of electrografted Ph–NO$_2$ interfaces that were deposited in the presence of increasing concentrations of DPPH. Interestingly, we observed multiple overlapping reduction peaks in the first reduction wave, indicating a polydispersity of chemical environments. The peak around −0.4 V becomes less prominent as the concentration of DPPH in the deposition medium increases, so that

only the more positive reduction peak at −0.2 V remains for interfaces grafted with 3 mmol/L DPPH. Similar features have previously been observed in CVs of electrografted Ph–NO$_2$ interfaces of varying thicknesses.[53] We attribute this to the presence of easily accessible species that are reduced at lower overpotentials (as would be the case in monolayer-like interfaces), and other species that are reduced with lower efficiencies at higher overpotentials e.g. due to a weaker distance-dependent electronic coupling, or inhibited diffusion of electrolyte into or through thicker interfaces. Indeed, the oxidation peak at 0.3 V vs RHE confirms the presence of partially-reduced Ph–NHOH species in these interfaces (*vide supra*). The relative ratio of this oxidation peak to the reduction peaks in the first reduction wave decreases as the DPPH scavenger concentration increases; further pointing to the deposition of fully accessible, thinner, monolayer-like interfaces.

To introduce a different surface chemistry at the ITO-electrolyte interface which is useful for the electrostatic immobilization of enzymes, and which can also eventually be activated for covalent immobilization *via* amide-coupling, carboxyphenyl (Ph–COOH) interfaces were also deposited on ITO from 1 mmol/L 4-carboxybenzene diazonium tetrafluoroborate (4-CBD) solutions in acetonitrile with and without the addition of 3 mmol/L DPPH.

To confirm the deposition of Ph–COOH interfaces as well as Ph–NO$_2$ interfaces and their subsequent reduction to Ph–NH$_2$ interfaces, IR spectroelectrochemical measurements were performed using a Kretschmann configuration in Attenuated Total Reflection (ATR) mode with a silicon prism, sputtered with a 20 nm thin coating of ITO (In$_2$O$_3$/SnO$_2$ 90/10 wt%). ATR-IR spectra recorded after electrografting from 4-NBD and 4-CBD solutions with DPPH scavenger (followed by thorough rinsing) are plotted in Figure 3. In both cases, a band around 1600 cm^{-1} is monitored, which corresponds to v(C=C) aromatic stretching vibrations of the phenyl moieties. v(NO$_2$) antisymmetric and symmetric stretching vibrations are observed at 1523 cm^{-1} and 1348 cm^{-1}, respectively, confirming the successful grafting of a Ph–NO$_2$ interface, while a v(C=O) stretching vibration at 1723 cm^{-1} confirms the successful electrografting of a Ph–COOH interface. IR spectra recorded after the electrochemical reduction of the Ph–NO$_2$ interface show an almost complete disappearance of the NO$_2$ stretching vibrations and the appearance of a band at 1514 cm^{-1} attributed to Ph–NH$_2$ groups.[31]

An ATR-IR difference spectrum recorded after incubating the Ph–COOH interface for several hours in a solution of N-(3-dimethylamino propyl)-N-ethylcarbodiimide hydrochloride (EDC) and N-hydroxysulfosuccinimide (sulfo-NHS) in PB at pH 5.5 is shown in Figure 3. The appearance of bands at 1742 and 1772 cm^{-1} corresponding to NHS-ester moieties confirm the successful activation of the surface and indicates that they are suitable for coupling with and subsequent covalent immobilization of enzymes.
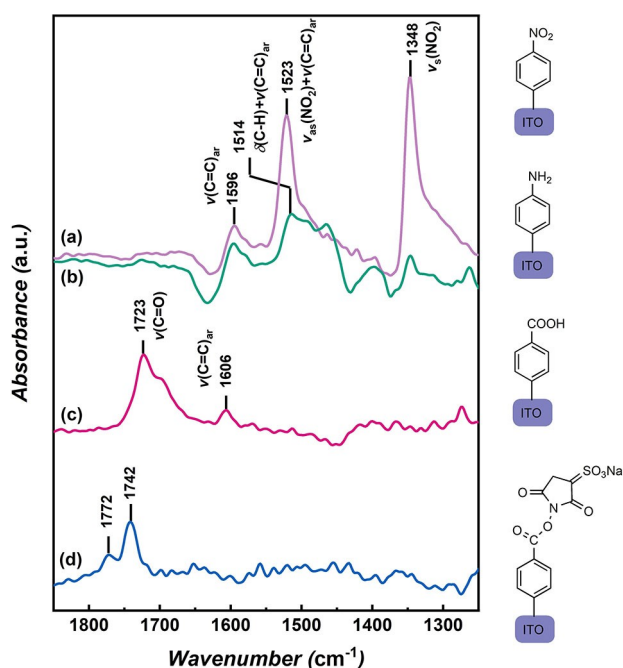
ChemElectroChem

Articles
doi.org/10.1002/celc.202100020

**Chemistry
Europe**

European Chemical
Societies Publishing

Figure 3. IR spectra recorded in ATR mode in acetonitrile of modified ITO with a) Ph−NO$_2$ interfaces electrografted from 1 mmol/L solution of 4-NBD with DPPH before and b) after electrochemical reduction to Ph−NH$_2$ species, as well as c) Ph−COOH interfaces electrografted from 1 mmol/L solution 4-CBD with DPPH. d) Spectrum showing the difference spectrum recorded in PB buffer of the Ph−COOH interface after and before reacting with an EDC/sulfo-NHS solution.

2.2. Enzyme Immobilization on Electrografted Interfaces

To determine the suitability of the electrografted interfaces for the immobilization of redox-active enzymes on ITO electrodes and the effect of using radical scavengers during electrografting, we investigated the H$_2$ oxidation activity of the immobilized oxygen-tolerant membrane-bound [NiFe]-hydrogenase (MBH) from the bacterium *Ralstonia eutropha* under turnover conditions. The amount of catalytic current depends

on the electroactive surface coverage of the enzyme, which in turn depends on the orientation of the enzyme and the structure of the interface (i.e. whether it is sufficiently thin to allow fast interfacial charge transfer).[55] Although the MBH possesses a weaker dipole moment than that of oxygen-sensitive [NiFe] hydrogenases,[30] we have previously demonstrated that it can be immobilized *via* electrostatic interactions in an oriented fashion on gold electrodes covered with either terminally-functionalized SAMs or an electrografted Ph−NH$_2$ interface.[30,31]

In the present case, the MBH, supplied in a phosphate-buffered solution, was immobilized onto electrografted ITO surfaces with different head groups, namely Ph−NH$_2$ and Ph−COOH.

Protein film voltammograms (PFVs) for the hydrogen oxidation reaction (HOR) of MBH immobilized on the different interfaces were recorded in H$_2$-saturated buffer at pH 5.5, where its inherent activity is highest[56] and the bound enzyme molecules experience still a certain electrostatic interaction. The determination of catalytic current densities in the absence or presence of the redox mediator methylene blue (MB) allowed to distinguish between direct electron transfer (i$_{DET}$) and DET in combination with mediated electron transfer (i$_{DET+MET}$), respectively.

For simplicity, Figure 4a shows only the PFVs recorded for MBH immobilized on Ph−NH$_2$/ITO interfaces deposited either in the absence or presence of 3 mmol/L of scavenger (for PFVs on interfaces deposited with all scavenger concentrations, see Figure S2). The sigmoidal shape of the voltammograms indicate the catalytic oxidation of H$_2$ with onset potentials close to the thermodynamic potential of H$_2$/H$^+$. At high potentials, a reversible, electrochemically induced inactivation of the MBH was observed.[57] Figure 4b shows i$_{DET}$ and i$_{DET+MET}$ as well as the ratio i$_{DET}$/i$_{DET+MET}$. The latter gives an indication of the relative amount of enzyme immobilized in a DET configuration. In fact, i$_{DET}$/i$_{DET+MET}$ increased from 0.14 without scavenger up to 0.83 with 3 mmol/L DPPH. Thus, at an interface made with 3 mmol/L DPPH, almost all of the MBH molecules were immobilized in a
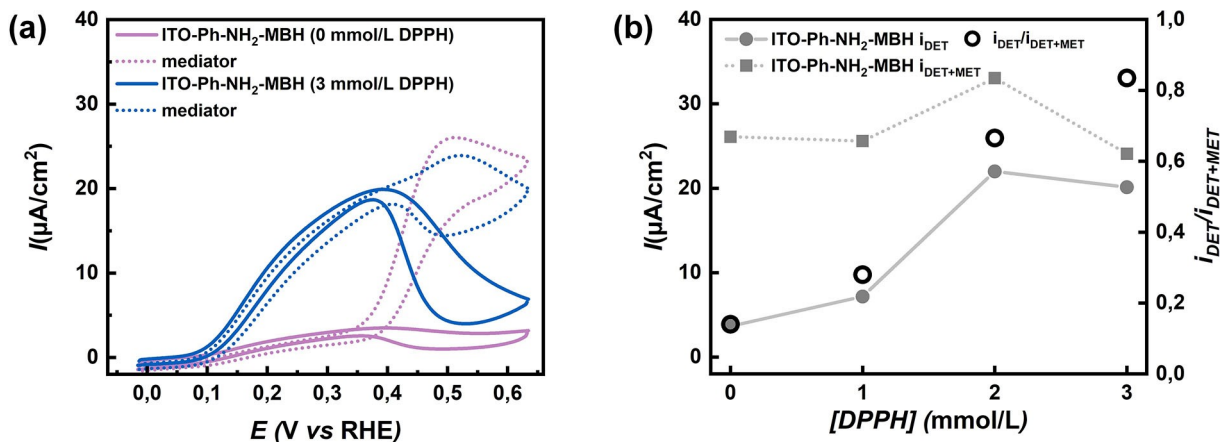

Figure 4. a) Representative protein film voltammograms (PFVs) recorded in H$_2$-saturated 10 mmol/L PB buffer of MBH adsorbed onto electrografted Ph−NH$_2$/ITO interfaces (deposited with and without addition of 3 mmol/L DPPH radical scavenger), before and after the addition of the redox mediator methylene blue. b) Plots of i$_{DET}$ and i$_{DET+MET}$ as a function of radical scavenger concentration added during electrografting of the Ph−NH$_2$/ITO interfaces.

ChemElectroChem

Articles
doi.org/10.1002/celc.202100020

**Chemistry
Europe**
European Chemical
Societies Publishing

DET configuration. Assuming that the orientation of the immobilized MBH remained stable on the different interfaces, and that only a monolayer of MBH was adsorbed on top of these interfaces (as proven for the MBH adsorbed on amine-functionalized SAMs[30]), the increasing DPPH concentrations led to electrografting of thinner interfaces. These, in turn, facilitated fast interfacial electron transfer. These results correlate perfectly to the electrochemical impedance spectroscopy findings described in section 1. In addition, onset potentials also shift closer to the potential of the H_2/H^+ couple for interfaces deposited with higher DPPH concentrations, along with open circuit potentials recorded under H_2 (see SI Figure S3). A similar effect was observed for the Ph–COOH interfaces (see SI Figure S3), where $i_{DET}/i_{DET+MET}$ increases from 0.29 without scavenger to 0.75 with 3 mmol/L DPPH.

The small differences between the current densities and $i_{DET}/i_{DET+MET}$ obtained on the final Ph–NH$_2$ and Ph–COOH interfaces may be explained by slightly different orientations adopted by the MBH molecules on these surfaces, different surface coverages or different effectiveness in controlling interfacial growth by the addition of radical scavengers as a result of different functional groups and a possible secondary mechanism. Indeed, Menanteau et al. showed that DPPH is effective in suppressing film growth *via* radical processes. However, film growth may still occur *via* aromatic substitution of diazonium ions or dediazoniated carbocations to already grafted species.[51] For strongly electron-withdrawing aryl substituents such as -NO$_2$, the former radical growth process prevails, while for less electron-withdrawing substituents such as –COOH, the latter may also occur. Nevertheless, we show that the utilization of a radical scavenger is still highly effective in controlling interface thickness on ITO, and more generally in maximizing DET for enzymes immobilized on two types of biocompatible electrografted interfaces.

To emphasize the challenges in immobilizing enzymes in a DET configuration on conductive oxides using chemical modification methods, we prepared aminopropyl-functionalized ITO electrodes, using silanes which are commonly used for enzyme immobilization. We employed both 3-aminopropyltriethoxysilane (APTES) and 3-aminopropyltrimethoysilane (APTMS), commonly used silanes for this purpose, and carefully followed procedures reported in literature.[10,18] The ITO slides were first cleaned and then dried at 150 °C and special care was taken to keep the toluene dry and to perform the functionalization under a protective N$_2$ atmosphere to prevent the deposition of thick interfaces due to polymerization/oligomerization. PFVs of MBH immobilized on these amino-functionalized, silanated interfaces are shown in Figure 5 and are compared to those obtained on the thinnest electrografted Ph–NH$_2$ interface (deposited with 3 mmol/L DPPH). No catalytic current resulting from DET was observed on the silane-derived interfaces, indicating that the silane-derived interfaces completely block interfacial charge transfer. Even in the presence of the mediator methylene blue, no current was observed for the APTES-derived ITO interface, and only a very low mediated current of 1.5 µA/cm^2 was recorded for the APTMS-modified ITO. These results may be explained by a faster hydrolysis rate of the methoxy
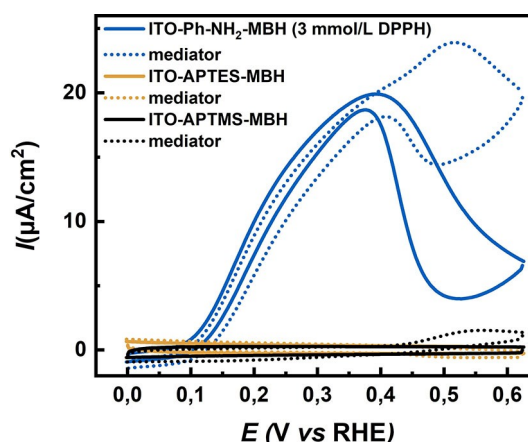

Figure 5. PFVs recorded in H$_2$-saturated buffer of MBH adsorbed on ITO modified with the silanes APTES and APTMS, as well as an electrografted Ph–NH$_2$ interface, before and after the addition of the redox mediator methylene blue.

groups during functionalization leading to a more polymeric and less dense interface that is permeable to the MB mediator.

2.3. Covalent Immobilization of Enzyme on Electrografted Interfaces

Covalent attachment prevents fast desorption or leaching of enzymes from an electrode surface (e.g. due to changes in pH) and thereby increase the stability of a device.[47,55,58] A common method for covalent attachment is to form amide bonds between functionalized surfaces and surface-exposed amino acid side chains of the enzymes.[27,42,59] To allow covalent attachment between the ITO and the α-amino groups of lysine residues on the surface of the MBH (~45 in total,[60] see SI Figure S4), ITO was electrografted with Ph–COOH (using 3 mmol/L DPPH). Ester formation for subsequent covalent attachment was achieved using 1-Ethyl-3-(3-dimethylaminopropyl)carbodiimide (EDC) and N-hydroxysulfosuccinimide (sulfo-NHS) in a 5:1 ratio. Afterwards MBH solution was added at a pH value of 5.5 as for the previously described immobilization of MBH on COOH-terminated SAM's (*vide supra*).

PFVs of the MBH-coated electrode in H$_2$ saturated electrolyte indicate that i_{DET} decreases by 50% in case of covalently attached MBH compared to the electrostatically adsorbed MBH (Figure 6b,c). This effect can have several reasons. The MBH molecules may adopt a random orientation on the EDC sulfo-NHS-activated surface because the lysine residues are distributed over the MBH surface or the interfacial charge transfer resistance has changed upon covalent attachment. Alternatively, the decrease in activity might be due to a loss of conformational flexibility upon covalent attachment. For covalently attached MBH, an $i_{DET}/i_{DET+MET}$ of 0.66 was obtained (SI Figure S5), which is comparable to the value of 0.75 obtained for electrostatically adsorbed MBH on the Ph–COOH interface.

Despite the lower catalytic current density, chronoamperometry (CA) measurements recorded at 0.43 V (vs RHE) shown

ChemElectroChem

Articles
doi.org/10.1002/celc.202100020

**Chemistry
Europe**
European Chemical
Societies Publishing

in Figure 6 (c) demonstrate that covalent attachment on ITO—Ph—COOH (see SI Figure S6 for CA measurements for all interfaces) led to an improved stability, i.e. the catalytic current density remained stable over a time period of 1.5 h. Comparing PFVs recorded before and after the CA measurements revealed a drop in i_{DET} of almost 20 % for MBH electrostatically immobilized on an ITO—Ph—COOH interface (3 mmol/L DPPH), whereas i_{DET} stayed stable in case of covalently attached MBH. We attribute this behavior to a higher surface stability of covalently bound MBH molecules, resulting in less desorption from the electrode surface.

3. Conclusions

Here we show that the electrografting of diazonium salt-based interfaces onto planar ITO electrodes can be controlled using a radical scavenger. The scavenger lowers the interface thickness, thereby enabling efficient DET of the electrode with an immobilized model enzyme, the oxygen-tolerant membrane-bound [NiFe]-hydrogenase (MBH) from *R. eutropha*. Amine and carboxylic acid functionalities relevant for enzyme immobilization were deposited using this approach mediating different interface charges that served as basis for enzyme immobilization under moderate electrostatic control. The electrografted

interfaces were also shown to be suitable for covalent immobilization of the MBH, leading to a significant improvement in current density stability compared to just electrostatically immobilized enzyme. Given the superior stability of the electrografted interfaces on metal oxides regarding to hydrolysis and desorption (as compared to interfaces deposited using conventional surface modification techniques), as well as the ability to easily control interface growth and maximize DET with the help of a radical scavenger, we propose our strategy to be an alternative approach for immobilizing enzymes on electrodes in bioelectronic devices. Recent work demonstrated successful electrografting on high-surface area nanostructures.[38–41] Our strategy should be extendable also to these materials.

Experimental Section

Electrochemical measurements were performed using either a CHI potentiostat or a Metrohm μAutolab II employing ITO glass slides as working electrodes (Sigma Aldrich, 8–12 Ω/sq), a Pt counter electrode, and either a Ag/AgCl 3 mol/L KCl (Dri-Ref, WPI) or a Ag/AgCl 3 mol/L KCl (Leak-Free, Warner Instruments) reference electrode for use in aqueous solvents or acetonitrile (CH_3CN, HPLC grade, Sigma-Aldrich), respectively. Potentials in aqueous solvents were converted to the reversible hydrogen electrode (RHE) using the Nernst equation ($E_{RHE} = E_{Ag/AgCl} + 0.059\ pH + E^{\circ}_{Ag/AgCl}$), whereas
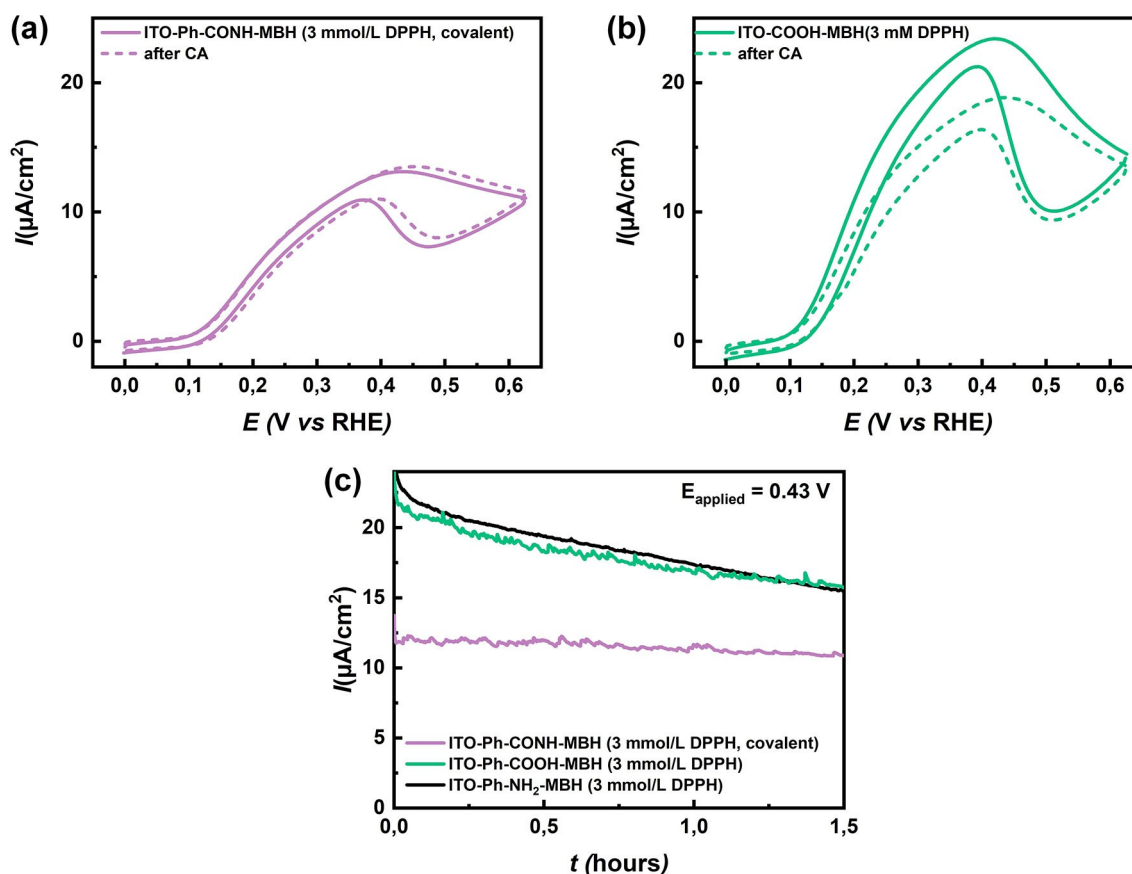

Figure 6. PFVs recorded in H_2-saturated buffer of MBH a) covalently or b) electrostatically immobilized on a Ph—COOH interface on ITO (3 mmol/L DPPH), before and after chronoamperometric measurements (CA) at an applied potential of 0.43 V (vs RHE), shown in (c). CA of MBH electrostatically immobilized on a Ph—NH₂ interface is also shown for comparison.

ChemElectroChem

Articles
doi.org/10.1002/celc.202100020

**Chemistry
Europe**
European Chemical
Societies Publishing

potentials in acetonitrile were measured and reported relative to the ferrocene/ferrocenium (Fc/Fc$^+$) redox couple. For all measurements and reactions in acetonitrile, a 0.1 mol/L tert-butylammonium perchlorate (TBAClO$_4$, Sigma-Aldrich) electrolyte was used. All electrochemical measurements, unless stated otherwise, were performed under inert argon atmosphere.

Prior to modification, the ITO electrodes were rinsed with water, dried, and then sonicated for 5 min in dichloromethane (CH$_2$Cl$_2$, Anhydrous, Sigma-Aldrich), before drying under a stream of N$_2$. Nitrophenyl (Ph–NO$_2$) and carboxyphenyl (Ph–COOH) interfaces were electrografted from 1 mmol/L 4-nitro-benzene diazonium tetrafluoroborate (4-NBD, Sigma-Aldrich) or 4-carboxybenzene diazonium tetrafluoroborate (4-CBD, synthesized using a published method[51]) solutions in acetonitrile using cyclic voltammetry, with and without the addition of increasing molar equivalents of 2,2-diphenyl-1-picrylhydrazyl (DPPH, Sigma-Aldrich) as radical scavenger. A custom-made PTFE electrochemical cell was used with FKM O-rings on the ITO slides forming a working electrode with a geometric surface area of 0.4 cm^2. Three consecutive cycles between 0.34 and −0.76 V (vs Fc/Fc$^+$) at a scan rate of 50 mVs^{-1} were used to electrograft Ph–NO$_2$ interfaces, and three consecutive cycles between 0.34 and −0.86 (vs Fc/Fc$^+$) were used to electrograft Ph–COOH interfaces, followed by rinsing the electrode in copious amounts of acetonitrile, dichloromethane (CH$_2$Cl$_2$) and ethanol (CH$_3$CH$_2$OH). For the covalent attachment, the N-hydroxysulfosuccinimide (sulfo-NHSS) ester was formed by exposure of the Ph–COOH interface to an aqueous solution of 75 mmol/L 1-ethyl-3-[3-(dimethylamino)propyl]carbodiimide hydrochloride (EDC, Sigma-Aldrich) and 15 mmol/L sulfo-NHSS (Sigma-Aldrich) at pH 7 for 1 h, afterwards an 1 μ mmol/L solution of MBH in 10 mM potassium phosphate buffer (PB) was incubated for 15 min at pH 5.5 and 5 °C.

Nitrophenyl (Ph–NO$_2$) interfaces were electrochemically reduced to aminophenyl (Ph–NH$_2$) interfaces by cycling the potential between 0.51 and −0.69 V (vs RHE) 10 times (scan rate 50 mVs^{-1}).

Aminopropyl-functionalized ITO electrodes were prepared by using 3-aminopropyl-triethoxysilane (APTES) and 3-aminopropyltrimethoxysilane (APTMS), following procedures reported in literature.[10,18] ITO slides were firstly cleaned and subsequently dried at 150 °C and transferred into toluene containing 1 % (v/v) APTES or APTMS under a nitrogen atmosphere and left to react overnight. Special care was taken to keep the toluene dry and to perform the functionalization under a protective N$_2$ atmosphere to prevent the deposition of thick interfaces due to polymerization/oligomerization. After modification, the electrodes were copiously rinsed with toluene, ethanol and finally water and dried with a stream of N$_2$.

Electrochemical impedance spectroscopy (EIS) measurements were carried out in a 1 mmol/L Fc solution in acetonitrile in the presence of 0.1 mol/L TBAClO$_4$ at 0 V (vs Fc/Fc$^+$) using a 20 mV sine-wave amplitude with a frequency range of 1 MHz to 0.01 Hz.

The heterodimeric, oxygen-tolerant membrane-bound [NiFe]-hydrogenase (MBH) from the "Knallgas" bacterium *Ralstonia eutropha*, carrying a *Strep*-tag II peptide, was purified by affinity chromatography as described elsewhere.[61]

For protein film voltammetry (PFV), MBH was immobilized on the modified ITO surfaces by incubating the ITO electrodes at 5 °C and 15 min in an 1 μmol/L solution of MBH in 10 mmol/L potassium phosphate buffer (PB) at either pH 7 for Ph–NH$_2$ interfaces or pH 5.5 for Ph–COOH interfaces. After incubation, electrodes were rinsed with PB, and PFV was performed in 10 mmol/L phosphate buffer at pH 5.5 and 25 °C with a scan rate of 10 mVs^{-1} after saturation of the electrolyte with O$_2$-free Ar or O$_2$-free H$_2$ gas, using an Agilent Gas Clean Oxygen Filter (CP17970).

ATR-IR measurements were performed in a Kretschmann configuration with an ITO-coated Si prism (for detailed description see[38]) and a homemade spectroelectrochemical cell operated at 25 °C (see Figure S7). For the ATR-IR measurements the about 20 nm thick ITO films were deposited onto the Si prism using a sputter-deposition-system from Bestec, Berlin. The sputtering time was 63 sec at a temperature of 350 °C in vacuum of 5.2 × 10^{-3} mbar and a distance from sample holder to sputter source of 75 mm. An Argon/oxygen atmosphere of 30 : 1 was used and the power of the RF was 200 W. A PTFE-coated O-ring was used to seal the electrochemical cell on top of the coated prism, forming a working electrode with a geometric surface area of 0.79 cm^2 in contact with the electrolyte.

IR Spectra were recorded between 4000 and 1000 cm^{-1} with a spectral resolution of 4 cm^{-1} on a Bruker IFS66v/s spectrometer equipped with a liquid N$_2$-cooled, photoconductive Mercury Cadmium Telluride detector. A temperature-controlled, homemade spectroelectrochemical cell was used at a controlled temperature of 25 °C. 400 scans were averaged per IR spectrum.

Conflict of Interest

The authors declare no conflict of interest.

[1] Y. Aksu, S. Frasca, U. Wollenberger, M. Driess, A. Thomas, *Chem. Mater.* **2011**, *23*, 1798–1804.

[2] S. Frasca, T. von Graberg, J. J. Feng, A. Thomas, B. M. Smarsly, I. M. Weidinger, F. W. Scheller, P. Hildebrandt, U. Wollenberger, *ChemCatChem* **2010**, *2*, 839–845.

[3] K. R. Stieger, S. C. Feifel, H. Lokstein, M. Hejazi, A. Zouni, F. Lisdat, *J. Mater. Chem. A* **2016**, *4*, 17009–17017.

[4] D. Mersch, C.-Y. Lee, J. Z. Zhang, K. Brinkert, J. C. Fontecilla-Camps, A. W. Rutherford, E. Reisner, *J. Am. Chem. Soc.* **2015**, *137*, 8541–8549.

[5] K. P. Sokol, D. Mersch, V. Hartmann, J. Z. Zhang, M. M. Nowaczyk, M. Rögner, A. Ruff, W. Schuhmann, N. Plumeré, E. Reisner, *Energy Environ. Sci.* **2016**, *9*, 3698–3709.

[6] S. Frasca, A. Molero Milan, A. Guiet, C. Goebel, F. Pérez-Caballero, K. Stiba, S. Leimkühler, A. Fischer, U. Wollenberger, *Electrochim. Acta* **2013**, *110*, 172–180.

[7] B. Neumann, P. Kielb, L. Rustam, A. Fischer, I. M. Weidinger, U. Wollenberger, *ChemElectroChem* **2017**, *4*, 913–919.

[8] K. J. Jetzschmann, A. Yarman, L. Rustam, P. Kielb, V. B. Urlacher, A. Fischer, I. M. Weidinger, U. Wollenberger, F. W. Scheller, *Colloids Surf. B* **2018**, *164*, 240–246.

[9] K. Peters, H. N. Lokupitiya, D. Sarauli, M. Labs, M. Pribil, J. Rathouský, A. Kuhn, D. Leister, M. Stefik, D. Fattakhova-Rohlfing, *Adv. Funct. Mater.* **2016**, *26*, 6682–6692.

[10] V. Müller, J. Rathousky, D. Fattakhova-Rohlfing, *Electrochim. Acta* **2014**, *116*, 1–8.

[11] I. H. Öner, C. J. Querebillo, D. David, U. Gernert, C. Walter, M. Driess, S. Leimkühler, K. H. Ly, I. M. Weidinger, *Angew. Chem. Int. Ed.* **2018**, *57*, 7225–7229; *Angew. Chem.* **2018**, *130*, 7344–7348.

[12] M. Miller, W. E. Robinson, A. R. Oliveira, N. Heidary, N. Kornienko, J. Warnan, I. A. C. Pereira, E. Reisner, *Angew. Chem. Int. Ed.* **2019**, *58*, 4601–4605.

[13] L. Yang, Y. Li, *Biosens. Bioelectron.* **2005**, *20*, 1407–1416.

[14] E. M. Oliveira, S. Beyer, J. Heinze, *Bioelectrochemistry* **2007**, *71*, 186–191.

[15] A. Facchetti, T. J. Marks, *Transparent Electronics*, John Wiley & Sons, Ltd, Chichester, UK, **2010**.

[16] M. G. Bellino, G. J. A. A. Soler-Illia, *Small* **2014**, *10*, 2834–2839.

[17] Y. Zhou, Y. Umasankar, R. P. Ramasamy, *J. Electrochem. Soc.* **2015**, *162*, H911–H917.

[18] E. González-Arribas, T. Bobrowski, C. Di Bari, K. Sliozberg, R. Ludwig, M. D. Toscano, A. L. De Lacey, M. Pita, W. Schuhmann, S. Shleev, *Biosens. Bioelectron.* **2017**, *97*, 46–52.

[19] M. Kato, T. Cardona, A. W. Rutherford, E. Reisner, *J. Am. Chem. Soc.* **2012**, *134*, 8332–8335.

[20] M. Kato, T. Cardona, A. W. Rutherford, E. Reisner, *J. Am. Chem. Soc.* **2013**, *135*, 10610–10613.

[21] D. Schaming, C. Renault, R. T. Tucker, S. Lau-Truong, J. Aubard, M. J. Brett, V. Balland, B. Limoges, *Langmuir* **2012**, *28*, 14065–14072.

[22] S. Shleev, E. González-Arribas, M. Falk, *Curr. Opin. Electrochem.* **2017**, *5*, 226–233.

[23] T. Bobrowski, E. González Arribas, R. Ludwig, M. D. Toscano, S. Shleev, W. Schuhmann, *Biosens. Bioelectron.* **2018**, *101*, 84–89.

[24] J. D. Benck, B. A. Pinaud, Y. Gorlin, T. F. Jaramillo, *PLoS One* **2014**, *9*, e107942.

[25] X. Fang, K. P. Sokol, N. Heidary, T. A. Kandiel, J. Z. Zhang, E. Reisner, *Nano Lett.* **2019**, *19*, 1844–1850.

[26] M. Mierzwa, E. Lamouroux, A. Walcarius, M. Etienne, *Electroanalysis* **2018**, *30*, 1241–1258.

[27] N. D. J. Yates, M. A. Fascione, A. Parkin, *Chem. A Eur. J.* **2018**, *24*, 12164–12182.

[28] A. Le Goff, M. Holzinger, *Sustain. Energy Fuels* **2018**, *2*, 2555–2566.

[29] V. P. Hitaishi, I. Mazurenko, M. Harb, R. Clément, M. Taris, S. Castano, D. Duché, S. Lecomte, M. Ilbert, A. De Poulpiquet, E. Lojou, *ACS Catal.* **2018**, *8*, 12004–12014.

[30] N. Heidary, T. Utesch, M. Zerball, M. Horch, D. Millo, J. Fritsch, O. Lenz, R. von Klitzing, P. Hildebrandt, A. Fischer, M. A. Mroginski, I. Zebger, *PLoS One* **2015**, *10*, e0143101.

[31] T. G. A. A. Harris, N. Heidary, J. Kozuch, S. Frielingsdorf, O. Lenz, M. Mroginski, P. Hildebrandt, I. Zebger, A. Fischer, *ACS Appl. Mater. Interfaces* **2018**, *10*, 23380–23391.

[32] A. Ciaccafava, P. Infossi, M. Ilbert, M. Guiral, S. Lecomte, M. T. Giudici-Orticoni, E. Lojou, *Angew. Chem. Int. Ed.* **2012**, *51*, 953–956; *Angew. Chem.* **2012**, *124*, 977–980.

[33] N. Kornienko, K. H. Ly, W. E. Robinson, N. Heidary, J. Z. Zhang, E. Reisner, *Acc. Chem. Res.* **2019**, *52*, 1439–1448.

[34] A. Forget, R. T. Tucker, M. J. Brett, B. Limoges, V. Balland, *Chem. Commun.* **2015**, *51*, 6944–6947.

[35] L. A. Martini, G. F. Moore, R. L. Milot, L. Z. Cai, S. W. Sheehan, C. A. Schmuttenmaer, G. W. Brudvig, R. H. Crabtree, *J. Phys. Chem. C* **2013**, *117*, 14526–14533.

[36] C. F. A. Negre, R. L. Milot, L. A. Martini, W. Ding, R. H. Crabtree, C. A. Schmuttenmaer, V. S. Batista, *J. Phys. Chem. C* **2013**, *117*, 24462–24470.

[37] R. Bangle, R. N. Sampaio, L. Troian-Gautier, G. J. Meyer, *ACS Appl. Mater. Interfaces* **2018**, *10*, 3121–3132.

[38] T. G. A. A. Harris, R. Götz, P. Wrzolek, V. Davis, C. E. Knapp, K. Ly, P. Hildebrandt, M. Schwalbe, I. Weidinger, I. Zebger, A. Fischer, *J. Mater. Chem. A* **2018**, *6*, 15200–15212.

[39] Y.-S. Kim, S. Fournier, S. Lau-Truong, P. Decorse, C. H. Devillers, D. Lucas, K. D. Harris, V. Balland, *ChemElectroChem* **2018**, *5*, 1625–1630.

[40] C. Wang, M. Amiri, R. T. Endean, O. Martinez Perez, S. Varley, B. Rennie, L. Rasu, S. H. Bergens, *ACS Appl. Mater. Interfaces* **2018**, *10*, 24533–24542.

[41] M. Dulac, A. Melet, K. D. Harris, B. Limoges, E. Galardon, V. Balland, *Sens. Actuators B* **2019**, *290*, 326–335.

[42] O. Rüdiger, J. M. Abad, E. C. Hatchikian, V. M. Fernandez, A. L. De Lacey, *J. Am. Chem. Soc.* **2005**, *127*, 16008–16009.

[43] G. Liu, J. J. Gooding, *Langmuir* **2006**, *22*, 7421–7430.

[44] C. Vaz-Dominguez, S. Campuzano, O. Rüdiger, M. Pita, M. Gorbacheva, S. Shleev, V. M. Fernandez, A. L. De Lacey, *Biosens. Bioelectron.* **2008**, *24*, 531–537.

[45] A. E. Radi, X. Munoz-Berbel, M. Cortina-Puig, J. L. Marty, *Electroanalysis* **2009**, *21*, 696–700.

[46] M. Pita, C. Gutierrez-Sanchez, D. Olea, M. Velez, C. Garcia-Diego, S. Shleev, V. M. Fernandez, A. L. De Lacey, *J. Phys. Chem. C* **2011**, *115*, 13420–13428.

[47] C. Baffert, K. Sybirna, P. Ezanno, T. Lautier, V. Hajj, I. Meynial-Salles, P. Soucaille, H. Bottin, C. Léger, *Anal. Chem.* **2012**, *84*, 7999–8005.

[48] S. Abdellaoui, B. C. Corgier, C. A. Mandon, B. Doumèche, C. A. Marquette, L. J. Blum, *Electroanalysis* **2013**, *25*, 671–684.

[49] T. Menanteau, E. Levillain, A. J. Downard, T. Breton, *Phys. Chem. Chem. Phys.* **2015**, *17*, 13137–13142.

[50] T. Menanteau, S. Dabos-Seignon, E. Levillain, T. Breton, *ChemElectroChem* **2017**, *4*, 278–282.

[51] T. Menanteau, M. Dias, E. Levillain, A. J. Downard, T. Breton, *J. Phys. Chem. C* **2016**, *120*, 4423–4429.

[52] T. Menanteau, E. Levillain, T. Breton, *Chem. Mater.* **2013**, *25*, 2905–2909.

[53] P. A. Brooksby, J. D. Shields, A. K. Farquhar, A. J. Downard, *ChemElectroChem* **2016**, *3*, 2021–2026.

[54] P. Brooksby, A. J. Downard, *J. Phys. Chem. B* **2005**, *109*, 8791–8798.

[55] J. A. Cracknell, K. A. Vincent, F. A. Armstrong, *Chem. Rev.* **2008**, *108*, 2439–2461.

[56] M. Ludwig, J. A. Cracknell, K. A. Vincent, F. A. Armstrong, O. Lenz, *J. Biol. Chem.* **2009**, *284*, 465–477.

[57] K. A. Vincent, A. Parkin, F. A. Armstrong, *Chem. Rev.* **2007**, *107*, 4366–4413.

[58] F. A. Al-Lolage, M. Meneghello, S. Ma, R. Ludwig, P. N. Bartlett, *ChemElectroChem* **2017**, *4*, 1528–1534.

[59] M. A. Alonso-Lomillo, O. Rüdiger, A. Maroto-Valiente, M. Velez, I. Rodríguez-Ramos, F. J. Muñoz, V. M. Fernández, A. L. De Lacey, *Nano Lett.* **2007**, *7*, 1603–1608.

[60] S. Frielingsdorf, J. Fritsch, A. Schmidt, M. Hammer, J. Löwenstein, E. Siebert, V. Pelmenschikov, T. Jaenicke, J. Kalms, Y. Rippers, F. Lendzian, I. Zebger, C. Teutloff, M. Kaupp, R. Bittl, P. Hildebrandt, B. Friedrich, O. Lenz, P. Scheerer, *Nat. Chem. Biol.* **2014**, *10*, 378–385.

[61] O. Lenz, L. Lauterbach, S. Frielingsdorf, *Enzym. Energy Technol.* (Ed.: F. B. T.-M. in E. Armstrong), Academic Press, **2018**, pp. 117–151.